DALTON
FULL PAPER

Synthesis and molecular structures of *N*,*N*-dimethylhydroxylamino-trichlorosilane and -germane †

Udo Losehand,[a] Norbert W. Mitzel*[a] and David W. H. Rankin[b]

[a] *Anorganisch-chemisches Institut, Technische Universität München, Lichtenbergstraße 4, 85747 Garching, Germany. E-mail: N.Mitzel@lrz.tum.de*
[b] *Department of Chemistry, University of Edinburgh, West Mains Road, Edinburgh, UK EH9 3JJ*

Received 18th August 1999, Accepted 13th October 1999

The compounds $Cl_3SiONMe_2$ and $Cl_3GeONMe_2$ have been prepared by reacting $HONMe_2$ with $SiCl_4$ and $GeCl_4$, respectively, in the presence of the auxiliary base 2,6-dimethylpyridine. Their identity was proven by gas-phase IR and solution NMR spectroscopy of the nuclei ^1H, ^{13}C, ^{15}N, ^{17}O, ^{29}Si, by mass spectrometry and elemental analyses. The solid-state structure of $Cl_3SiONMe_2$ was determined by low-temperature X-ray crystallography. The molecular structures of $Cl_3SiONMe_2$ and $Cl_3GeONMe_2$ in the gas phase have been determined by analysis of electron diffraction data augmented by restraints derived from *ab initio* calculations (MP2/6-31G*). The molecules adopt C_s symmetry. Important gas-phase geometry parameter values for $Cl_3SiONMe_2$ are: Si–O 1.623(3), Si–$Cl_{in\text{-}plane}$ 2.022(4), Si–$Cl_{out\text{-}of\text{-}plane}$ 2.024(2), O–N 1.479(6) Å, Si–O–N 105.6(8), O–Si–$Cl_{in\text{-}plane}$ 104.2(3), O–Si–$Cl_{out\text{-}of\text{-}plane}$ 113.7(2)°, for $Cl_3GeONMe_2$: Ge–O 1.759(6), Ge–$Cl_{in\text{-}plane}$ 2.104(4), Ge–$Cl_{out\text{-}of\text{-}plane}$ 2.106(2), O–N 1.484(9) Å, Ge–O–N 104.0(11), O–Ge–$Cl_{in\text{-}plane}$ 108.9(20), O–Ge–$Cl_{out\text{-}of\text{-}plane}$ 111.6(12)°. The structural data are interpreted in terms of weak attractive interactions between the nitrogen donor and the silicon/germanium acceptor atoms. The results are discussed in comparison with other structural data from the literature: the donor–acceptor interaction in $Cl_3SiONMe_2$ is weaker than those in $H_3SiONMe_2$ or $ClH_2SiONMe_2$, but stronger than that in $Me_3SiON(CF_3)_2$. Both compounds reveal stronger donor–acceptor interactions than the methyl analogues $Me_3SiONMe_2$.

Introduction

Silanes and germanes reveal Lewis acidic character depending on the nature of their substituents. The hypervalent base adducts have been intensively investigated[1] and some of them are of pharmaceutical interest.[2] Compounds with intramolecular donor–acceptor bonds form an important subset, and the best known class of compounds in this respect is the silatranes.[3] Driving the intramolecular donor–acceptor bond formation to the extreme of only one linker atom between donor and acceptor, three-membered rings can be formed or, as an alternative, oligomerisation can occur to give six-membered or larger ring systems.

We have studied internal donor–acceptor bond formation between E and N in E–O–N fragments (E = Si, Ge, Sn) and found a wide spectrum of strength of such interactions ranging from predictably weak ones *e.g.* in $Me_3SiONMe_2$ [Si–N: 2.566(8) Å, Si–O–N: 107.9(6)°][4] and its germanium analogue, through medium strength interactions *e.g.* in $H_2Si(ONMe_2)_2$ [Si–N: 2.32 Å, Si–O–N: 95°],[5] to strong interactions as in the solid state of $ClH_2SiONMe_2$ [Si–N: 2.028(1) Å, Si–O–N: 79.7(1)°].[6] In none of these compounds do we observe aggregation to six-membered ring systems, but instead we find a preference for formation of three-membered rings with one weak bond, which may be described as a donor–acceptor interaction with a large electrostatic contribution.

The determination of interactions of this type is important to understand specific reactivity of Si–O–N compounds, such as their rearrangements into O–N–Si units,[7] the use of catalytic amounts of R_2NOH in the alcoholysis reaction of Si–H functions[8] (also known in a stoichiometric version)[9] or their use as so-called cold-curing catalysts in silicone polymer synthesis.[10]

The principal concept of attractive interactions between geminal centres can be seen in a more general context. For example, interactions of this type have also been postulated for E–C–N linkages (E = Si, Ge, Sn; *e.g.* in $Me_3SnCH_2NMe_2$), and were used to explain the unusually low basicities of such amines (also named the α-effect).[11] However, they could not be proved on the basis of experimental structure determination to date.[12] Other examples from the literature in p-block element chemistry include the compounds $(F_3C)_2BCPh_2NMe_2$, R N=C{Al[CH(SiMe$_3$)$_2$]}$_2$ and $(Me_3Si)_2C{=}N{-}N\{Al[CH(SiMe_3)_2]\}_2$ with B–C–N,[3] Al–C=N[4] and Al–N–N[5] linkages forming three-membered ring systems in the solid state. In contrast to the limited number of examples of β-donor interactions in p-block chemistry, such a bonding situation is much more common in transition metal compounds like $Ti(ONR_2)_4$.[13] In these cases this type of bonding is also described as η^2-coordination.

For the bonding situation in Si–O–N units we know that the nucleophilic character of the nitrogen centre is of crucial importance, as has been shown in two recent studies of compounds with reduced basicity at nitrogen: $Me_3SiON(CF_3)_2$[14] and $(Mes)F_2SiON(SiMe_3)_2$.[15] We now wanted to evaluate the importance of backbonding from substituents to the acceptor atoms in Si–O–N and Ge–O–N compounds. In comparison to $ClH_2SiONMe_2$, with its exceptionally strong Si···N interaction, we aimed to prepare and study compounds with a larger number of Cl substituents at Si and Ge. Here we report on the synthesis of $Cl_3SiONMe_2$ and $Cl_3GeONMe_2$, and studies of their spectroscopic and structural properties.

† Dedicated to Professor H. Schmidbaur on the occasion of his 65th birthday.

Supplementary data available: rotatable 3-D crystal structure diagram in CHIME format. See http://www.rsc.org/suppdata/dt/1999/4291/

Also available: correlation matrix elements for Cl_3EONMe_2 (E = Si, Ge). For direct electronic access see http://www.rsc.org/suppdata/dt/1999/4291/, otherwise available from BLDSC (No. SUP 57668, 2 pp.) or the RSC Library. See Instructions for Authors, 1999, Issue 1 (http://www.rsc.org/dalton).

Table 1 NMR chemical shifts (ppm) of different *O*-silylated and *O*-germylated hydroxylamines

Compound	δ^{29}Si	δ^{15}N	δ^{17}O
$Cl_3SiONMe_2$	−42.4	−229.4	161
$Cl_3GeONMe_2$		−226.7	187
$Me_3SiONMe_2$	−17.8	−247.8	−13
$Me_3GeONMe_2$		−250.8	146
$H_3SiONMe_2$	−40.0	−234.0	112

Results and discussion

Synthesis and characterisation of $Cl_3SiONMe_2$ and $Cl_3GeONMe_2$

The compounds $Cl_3SiONMe_2$ and $Cl_3GeONMe_2$ were prepared by the reaction of *N*,*N*-dimethylhydroxylamine and the corresponding Group 14 tetrachloride in pentane in the presence of 2,6-dimethylpyridine as a non-coordinating hydrogen chloride acceptor.

$$ECl_4 + HONMe_2 + 2,6\text{-}Me_2C_5H_3N \longrightarrow Cl_3EONMe_2 + 2,6\text{-}Me_2C_5H_3N{\cdot}HCl,\ E = Si, Ge$$

They were isolated as colourless liquids by fractionation through a series of cold traps. Both $Cl_3SiONMe_2$ and $Cl_3GeONMe_2$ are extremely sensitive to moist air. $Cl_3GeONMe_2$ is thermally unstable and decomposes rapidly at ambient temperature to give $GeCl_4$ and the thermodynamically favoured $Cl_2Ge(ONMe_2)_2$. The chemical properties and molecular structure of $Cl_2Ge(ONMe_2)_2$ have been described elsewhere.[16]

$$2\ Cl_3GeONMe_2 \longrightarrow GeCl_4 + Cl_2Ge(ONMe_2)_2$$

The identity of $Cl_3SiONMe_2$ and $Cl_3GeONMe_2$ was proven by NMR spectroscopy (^{1}H, ^{13}C, ^{15}N, ^{17}O, and ^{29}Si for $Cl_3SiONMe_2$) and gas-phase IR spectroscopy. Owing to the high air sensitivity and thermal instability of $Cl_3GeONMe_2$, results from mass spectrometry and elemental analysis appeared only to be satisfactory in the case of $Cl_3SiONMe_2$.

Table 1 contains important NMR data for $Cl_3SiONMe_2$ and $Cl_3GeONMe_2$. The electronegative chlorine substituents in $Cl_3SiONMe_2$ lead to a shift of the ^{29}Si NMR signal to low frequency (δ −42.4), compared to the hydrogenated and methylated species $H_3SiONMe_2$ (δ −40.0) and $Me_3SiONMe_2$ (δ −17.8), respectively. The ^{15}N NMR resonances of $Cl_3SiONMe_2$ (δ −229.4) and $Cl_3GeONMe_2$ (δ −226.7) are shifted about 20 ppm to high frequency relative to $Me_3SiONMe_2$ (δ −247.8) and $Me_3GeONMe_2$ (δ −250.8), which may indicate a more intense interaction with the acceptor atoms silicon and germanium, respectively. The similarity in the chemical shifts gives further evidence of the similar electronic nature of the nitrogen atoms in $Cl_3SiONMe_2$ and $Cl_3GeONMe_2$.

In contrast to the extremely different ^{17}O NMR chemical shifts of the methylated compounds $Me_3SiONMe_2$ and $Me_3GeONMe_2$ at δ −13 and 146, the ^{17}O NMR resonances of $Cl_3SiONMe_2$ and $Cl_3GeONMe_2$ appear at similar chemical shifts (δ 161 and 187) and are the highest chemical shifts obtained for *O*-silylated and *O*-germylated hydroxylamines.

Crystal structure determination

In order to compare molecular geometries derived from gas-phase electron diffraction with solid-state geometries a single crystal of $Cl_3SiONMe_2$ was grown directly from the melt by *in situ* methods. Attempts to perform an analogous experiment for $Cl_3GeONMe_2$ failed due to problems with crystallisation. $Cl_3SiONMe_2$ crystallises with two independent molecules in the unit cell. There are no intermolecular contacts which would normally be regarded as significant. Important geometrical parameter values are listed in Table 2. Both molecules show a distorted tetrahedral geometry at the silicon centre due to an intramolecular donor–acceptor interaction between silicon and nitrogen (Fig. 1). These Si · · · N β-donor–acceptor interactions lead to small Si · · · N distances of 2.441(2) and 2.432(2) Å and markedly compressed Si–O–N angles of 103.4(1) and 102.6(1)°. Surprisingly, the Si · · · N β-donor–acceptor interactions in this case and in $H_3SiONMe_2$ [Si–O–N 102.6(1)°, Si · · · N 2.456(1) Å] are very similar, whereas in $ClH_2SiONMe_2$ the Si–O–N angle is 24° less and the Si · · · N distance is 0.41 Å shorter. Moreover, this is despite the fact that $H_3SiONMe_2$ and $ClH_2SiONMe_2$ are both compounds with a less electrophilic silicon centre, or in other words with a less positive charge at the silicon atom, which could be expected to lead to a stronger electrostatic attraction between Si and N atoms in $Cl_3SiONMe_2$.

Table 2 Important crystal structure parameter values (distances/Å, angles/°) for the two independent molecules of $Cl_3SiONMe_2$ in the unit cell

Parameter	Molecule 1	Molecule 2
Si–O	1.618(2)	1.622(2)
Si–Cl4	2.018(1)	2.018(1)
Si–Cl5	2.015(1)	2.022(1)
Si–Cl6	2.013(1)	2.018(1)
O–N	1.491(2)	1.493(2)
N–C7	1.462(4)	1.461(3)
N–C8	1.455(4)	1.457(3)
Si–O–N	103.4(1)	102.6(1)
O–Si–Cl4	104.2(1)	104.3(1)
O–Si–Cl5	113.5(1)	113.3(1)
O–Si–Cl6	113.3(1)	113.5(1)
O–N–C7	104.2(2)	104.7(2)
O–N–C8	104.5(2)	104.7(2)

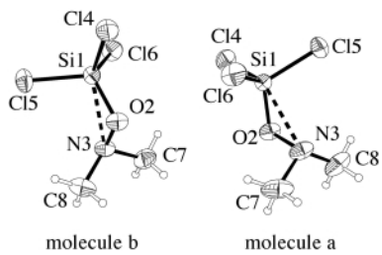

Fig. 1 Crystal structure of $Cl_3SiONMe_2$ as determined by low-temperature crystallography with numbering scheme for the two independent molecules in the asymmetric unit. The molecules are shown in their relative orientation towards each other in the crystal lattice.

The N–O bond length [1.492(ave) Å] is significantly elongated with respect to the non-silylated $HONMe_2$ [1.452(ave) Å], but of the same length as in $ClH_2SiONMe_2$ [1.490(1) Å]. A marked distortion of the coordination sphere of silicon is obvious from the different O–Si–Cl angles, with the angle in the (pseudo-)plane of symmetry being about 104°, while the other two are widened to more than 113° in both independent molecules. This and the other parameter values justify the silicon atom in $Cl_3SiONMe_2$ being regarded as (4 + 1)-coordinate.

Gas-phase structure determination

The high volatility of both $Cl_3SiONMe_2$ and $Cl_3GeONMe_2$ allowed the determination of their molecular structures in the gas phase by means of electron diffraction. In supporting the refinement by restraints derived from *ab initio* geometry optimisations the usual limitations of gas-phase structure refinements can be overcome. This procedure is called the SARACEN method[17] and introduces an elaborate combination of Bartell's method of predicating values[18] and Schäfer's MOCED method.[19]

Table 3 Geometrical parameter values and restraints for the GED refinements of $Cl_3SiONMe_2$ and $Cl_3GeONMe_2$. The parameter values from the *ab initio* calculations (MP2/6-31G*) are listed for comparison. Distances are given in Å, angles and torsion angles in °

		$Cl_3SiONMe_2$			$Cl_3GeONMe_2$		
No.	Parameter	Value	Restraint	MP2/6-31G*	Value	Restraint	MP2/6-31G*
*p*1	E–Cl4	2.022(4)		2.034	2.104(4)		2.129
*p*2	E–Cl5/6	2.024(2)	*p*2 − *p*1 = 0.001(5)	2.035	2.106(2)	*p*2 − *p*1 = 0.001(5)	2.130
*p*3	E–O	1.623(3)		1.663	1.759(6)		1.789
*p*4	O–N	1.479(6)		1.492	1.484(9)		1.500
*p*5	N–C7	1.445(4)	*p*5 − *p*4 = 0.031(10)	1.461	1.447(7)	*p*5 − *p*4 = 0.040(10)	1.460
*p*6	C7–H9	1.142(9)		1.089	1.095(21)		1.090
*p*7	C7–H10	1.146(9)	*p*7 − *p*6 = 0.004(5)	1.093	1.098(22)	*p*7 − *p*6 = 0.003(5)	1.093
*p*8	C7–H11	1.150(9)	*p*7 − *p*6 = 0.008(5)	1.097	1.101(22)	*p*7 − *p*6 = 0.007(5)	1.097
*p*9	O–E–Cl4	104.2(3)		104.1	108.9(20)		108.9
*p*10	E–O–N	105.6(8)		100.4	104.0(11)		95.6
*p*11	O–N–C	107.0(5)	2 × *p*11 + *p*12 = 320.6(30)	104.5	106.3(9)	2 × *p*11 + *p*12 = 320.8(30)	104.5
*p*12	C7–N–C8	114.9(7)	*p*12 − *p*11 = 7.10(10)	111.6	114.1(11)	*p*12 − *p*11 = 7.4 (10)	111.9
*p*13	O–E–Cl5/6	113.7(2)		113.0	111.6(12)		112.9
*p*14	N–C7–H9	107.9(9)	*p*14 = 108.9(10)	108.9	108.1(10)	*p*14 = 108.9(10)	108.9
*p*15	N–C7–H10	106.5(10)	*p*15 − *p*14 = 1.5(5)	107.4	106.9(11)	*p*15 − *p*14 = 1.2(5)	107.7
*p*16	N–C7–H11	110.2(10)	*p*16 − *p*14 = 2.5(5)	111.4	110.5(11)	*p*16 − *p*14 = 2.4(5)	111.2
*p*17	τC–N–C–H9	−198.1(31)		−176.8	−197.5(89)		−177.2
*p*18	τC–N–C–H10	41.9(27)	*p*18 − *p*17 = 241.9(30)	65.1	44.5(89)	*p*18 − *p*17 = 241.8(30)	64.6
*p*19	τC–N–C–H11	−76.6(32)	*p*19 − *p*17 = 121.4(30)	−55.4	−77.0(90)	*p*19 − *p*17 = 121.2(30)	−56.0
*p*20	τN–O–E–Cl5	60.6(5)		62.5	58.9(37)		62.1

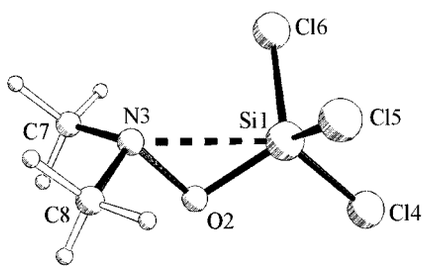

Fig. 2 Molecular structure of $Cl_3SiONMe_2$ in the gas phase as determined by electron diffraction with numbering scheme. The structure of $Cl_3GeONMe_2$ is similar, the numbering scheme analogous.

The molecular framework and atom numbering scheme for $Cl_3SiONMe_2$ and $Cl_3GeONMe_2$ are shown in Fig. 2. The mathematical model for the least squares refinement of both compounds was defined in C_s symmetry, with six bond lengths: E–O, E–Cl4, E–Cl5, O–N, N–C and one C–H distance for the methyl groups bound to nitrogen. The differences between the C–H distances within these groups were restrained to the values obtained from *ab initio* calculations at the MP2/6-31G* level of theory. Parameters for refinement were the angles O–E–Cl4, O–E–Cl5/6, E–O–N, O–N–C, C–N–C, and the angles N–C–H as well as the torsion angles τNOECl5 and τCNCH, whereby the differences between parameters for the different hydrogen atoms were again restrained to calculated values. In all 20 geometry parameters were refined under the action of 10 restraints defining the differences of parameters of similar nature or absolute values in the case of hydrogen-defining parameters. The parameter and restraint definitions are given in Table 3; the uncertainties are based on experience with the reliability of these calculations. Also 21 amplitudes of vibration were refined concurrently, representing all amplitudes belonging to pairs of scatterers with a contribution of more than 5% of the scattering of the E–Cl pair. Most of these amplitudes were subject to restraints, either absolute or ratios between related amplitudes, with the values taken from a force field computed at the MP2/6-31G* level of theory and transformed into amplitudes by means of the program ASYM40[13] after scaling it by an overall factor of 0.93, which is an established constant in our laboratories. These amplitudes and restraints are given in Table 4. The quality of the refinement can be assessed from the residuals in the molecular scattering curves (Fig. 3) and the radial distribution curves (Fig. 4). The final *R* factors

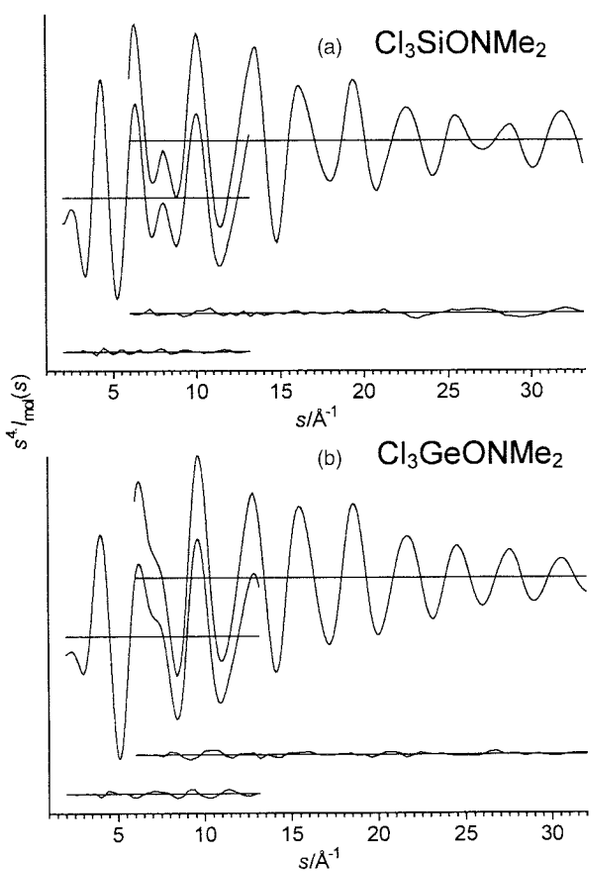

Fig. 3 Experimental molecular scattering intensity and final difference curves (*vs.* model) as obtained by electron diffraction of (a) gaseous $Cl_3SiONMe_2$ and (b) gaseous $Cl_3GeONMe_2$ (including the contribution of $GeCl_4$).

were 0.053 and 0.052 for $Cl_3SiONMe_2$ and $Cl_3GeONMe_2$. The gas-phase structure of $Cl_3GeONMe_2$ was obtained from a mixture of the compound with $GeCl_4$, and the scattering contribution of $GeCl_4$ was treated by including its known gas-phase geometry in the model. The ratio $Cl_3GeONMe_2$:$GeCl_4$ was found to be 52:48% by variation of the composition parameter in the refinement and an uncertainty of ±5% was estimated by a Hamilton test at the 95% confidence level. Variation of the

Table 4 Distances, amplitudes of vibration and restraints for the GED refinements of the compounds $Cl_3SiONMe_2$ and $Cl_3GeONMe_2$. Distances and amplitudes are given in Å

		$Cl_3SiONMe_2$			$Cl_3GeONMe_2$		
No.	Atom pair	Distance	Amplitude	Restraint	Distance	Amplitude	Restraint
*d*1	E–Cl4	2.022(4)	0.047(2)		2.104(4)	0.043(3)	
*d*2	E–Cl5	2.024(2)	0.047(1)	*u*2/*u*1 = 0.996(50)	2.106(2)	0.043(3)	*u*2/*u*1 = 0.998(50)
*d*3	E–O2	1.623(3)	0.044(4)	*u*3/*u*1 = 0.949(95)	1.759(6)	0.040(3)	*u*3/*u*1 = 0.917(46)
*d*4	O2–N3	1.479(6)	0.049(4)		1.484(9)	0.055(5)	0.054(54)
*d*5	N3–C7	1.445(4)	0.045(4)	*u*5/*u*4 = 0.928(46)	1.447(7)	0.050(5)	*u*5/*u*4 = 0.908(45)
*d*6	C7 · · · H9	1.142(9)	0.083(6)	0.078(8)	1.095(22)	0.081(7)	0.077(8)
*d*7	C7 · · · H10	1.146(9)	0.084(7)	*u*7/*u*6 = 1.005(50)	1.098(22)	0.081(8)	*u*7/*u*6 = 1.005(50)
*d*8	C7 · · · H11	1.150(9)	0.085(7)	*u*8/*u*6 = 1.014(51)	1.101(22)	0.082(9)	*u*8/*u*6 = 1.014(51)
*d*9	Cl4 · · · Cl5	3.309(8)	0.076(7)		3.440(72)	0.107(32)	
*d*10	Cl5 · · · Cl6	3.228(18)	0.076(9)	*u*10/*u*9 = 0.998(50)	3.355(153)	0.107(32)	*u*10/*u*9 = 1.001(50)
*d*11	Cl4 · · · O2	2.886(5)	0.074(7)		3.150(40)	0.096(10)	0.102(10)
*d*12	Cl4 · · · N3	4.218(9)	0.098(9)		4.429(25)	0.109(10)	0.104(10)
*d*13	Cl4 · · · C7	5.018(9)	0.151(11)		5.245(31)	0.145(12)	0.137(14)
*d*14	Cl5 · · · O2	3.061(3)	0.072(6)	*u*14/*u*11 = 0.978(49)	3.202(23)	0.095(9)	0.099(10)
*d*15	Cl5 · · · N3	3.302(12)	0.168(13)	0.161(16)	3.372(27)	0.160(16)	0.156(16)
*d*16	Cl5 · · · C7	4.623(11)	0.139(9)		4.699(33)	0.155(15)	0.168(17)
*d*17	Cl5 · · · C8	3.675(18)	0.216(17)	0.219(32)	3.733(37)	0.223(21)	0.216(22)
*d*18	E · · · N3	2.473(12)	0.131(10)		2.562(17)	0.098(11)	0.117(12)
*d*19	E · · · C7	3.445(10)	0.131(11)	0.124(12)	3.537(17)	0.130(11)	0.123(12)
*d*20	O2 · · · C7	2.351(8)	0.075(6)	*u*20/*u*18 = 0.571(57)	2.346(15)	0.080(7)	0.072(7)
*d*21	C7 · · · C8	2.437(12)	0.075(9)	*u*21/*u*18 = 0.577(58)	2.428(18)	0.069(7)	0.069(7)
*d*22	Cl4 · · · H9	4.601(27)	0.241	(fixed)	4.836(49)	0.246	(fixed)
*d*23	Cl4 · · · H10	5.449(42)	0.153	(fixed)	5.652(142)	0.164	(fixed)
*d*24	Cl4 · · · H11	5.980(25)	0.240	(fixed)	6.144(64)	0.243	(fixed)
*d*25	Cl5 · · · H9	4.772(22)	0.214	(fixed)	4.855(51)	0.215	(fixed)
*d*26	Cl5 · · · H10	5.343(22)	0.255	(fixed)	5.388(39)	0.260	(fixed)
*d*27	Cl5 · · · H11	5.116(32)	0.166	(fixed)	5.150(79)	0.169	(fixed)
*d*28	Cl6 · · · H9	3.068(38)	0.284	(fixed)	3.144(89)	0.282	(fixed)
*d*29	Cl6 · · · H10	4.664(31)	0.311	(fixed)	4.671(79)	0.318	(fixed)
*d*30	Cl6 · · · H11	4.125(57)	0.241	(fixed)	4.129(149)	0.239	(fixed)

$Cl_3GeONMe_2$: $GeCl_4$ ratio about the optimised value in this range did not affect the geometric parameters of $Cl_3GeONMe_2$ significantly.

$Cl_3SiONMe_2$ and $Cl_3GeONMe_2$ adopt similar molecular structures in the vapour. Each of the compounds shows a compressed E–O–N angle, 105.6(8)° for $Cl_3SiONMe_2$ and 104.0(11)° for $Cl_3GeONMe_2$, which leads to short E · · · N distances [E = Si: 2.473(12) Å, E = Ge: 2.562(17) Å]. The N→E donor–acceptor interaction results in a distortion of the tetrahedral coordination geometry, which is more pronounced in $Cl_3SiONMe_2$ [O–Si–Cl angles 104.2(3) and 113.7(2)°] than in $Cl_3GeONMe_2$ [O–Ge–Cl angles 108.9(20) and 111.6(12)°]. Angles and distances of relevance are given in Table 3.

Comparison of the results derived from gas-phase electron diffraction and X-ray diffraction of a single crystal of $Cl_3SiONMe_2$ shows that both molecular structures are similar. The distortion of the tetrahedral coordination geometry at the silicon centre is, within experimental errors, the same for both gas-phase and crystal structures. $Cl_3SiONMe_2$ adopts slightly smaller Si–O–N angles in the crystal than in the vapour. This was expected with respect to the known structure of the *anti*-conformer of $ClH_2SiONMe_2$ [Si–O–N: gas phase 87.1(9)°; crystal lattice 79.1(1)°].[6] The compression of the Si–O–N angle in the solid state is explained by the increase of the molecular dipole moment due to the regular alignment of the molecules in the crystal lattice.

Ab initio calculations at the MP2(fc)/6-31G* level of theory overestimate the strength of the Si · · · N interaction: $Cl_3SiONMe_2$ is predicted to have a significantly smaller E–O–N angle (100.4°), implying a stronger donor–acceptor interaction than found by experiment. This overestimation of the strength of the E · · · N β-donor interaction is even more pronounced for $Cl_3GeONMe_2$, for which the Ge–O–N angle is computed 8° smaller (95.6°) than the experimental value of 104.0(11)° and the coordination tetrahedron at the germanium centre is less distorted than anticipated by theory (MP2/6-31G*). It is known from earlier comparison of experiments with theory that an improvement in the basis set leads to better values, but so far we have not observed such large deviations. A summary of theoretical and experimental bond lengths and angles is given in Table 3.

In order to improve understanding of the bonding situation in the title compounds, it is worth comparing them with other compounds containing X_3SiO linkages. Selected parameter values for reference compounds are given in Table 5. The Si–O bond in $Cl_3SiONMe_2$ [1.632(3) Å] is longer than in $Cl_3SiOSiCl_3$ [1.592(10) Å][20] or the fluorine analogue $F_3SiOSiF_3$ [1.580(25) Å].[21] This is consistent with the much narrower valence angle at oxygen in $Cl_3SiONMe_2$ [105.6(8)°] as compared to these disiloxanes [146(4) and 155.7(20)°], as the strength of a Si–O bond is related to a contribution of the oxygen lone pairs of electrons, which is more correlated with the width of the angle at oxygen. However, compounds without electronegative substituents at silicon have longer Si–O bonds, as is the case in $H_3SiOSiH_3$ and H_3SiOCH_3 (see Table 5). The variation in the Si–O–X angle from Si–O–Si to Si–O–C to Si–O–N angle is impressive and illustrates the importance of interactions between geminal atoms, which is repulsive in Si–O–Si, about neutral in Si–O–C and attractive in Si–O–N units.

We also wanted to compare our new experimental results with data for related Group 14 hydroxylamino compounds. For this purpose we prepared Table 6, which contains a collection of geometrical data and the corresponding values of the sums of Bartell's one angle radii [these radii define the (non-bonded) distance between geminal atoms, *i.e.* the A · · · C distance in an A–B–C unit enclosing one angle],[22] giving an estimate of the non-bonded distance between two geminal atoms bound to a common centre. The table shows that, depending on the substitution pattern, it is possible to achieve an E · · · N distance in E–O–N units which is identical to the sum of Bartell's radii indicating the absence of any attractive interaction, as in $MesF_2SiON(SiMe_3)_2$. However, it is also possible to achieve

Table 5 Important gas-phase geometrical parameter values (distances/Å, angles/°) for $Cl_3SiONMe_2$, $Cl_3GeONMe_2$ and other E–O–E and E–O–C reference compounds (GED values all r_a)

Compound	E–O	E–O–X
$Cl_3SiONMe_2$	1.623(3)	105.6(8)
$Cl_3SiOSiCl_3$	1.592(10)	146(4)
$F_3SiOSiF_3$	1.580(25)	155.7(20)
F_3SiOCH_3[31]	1.580(assumed)	131.4(32)
$H_3SiOSiH_3$	1.634(2)	144.1(8)
H_3SiOCH_3	1.640(3)	120.6(10)
$Cl_3GeONMe_2$	1.759(6)	104.0(11)
$H_3GeOGeH_3$	1.766(4)	126.5(3)

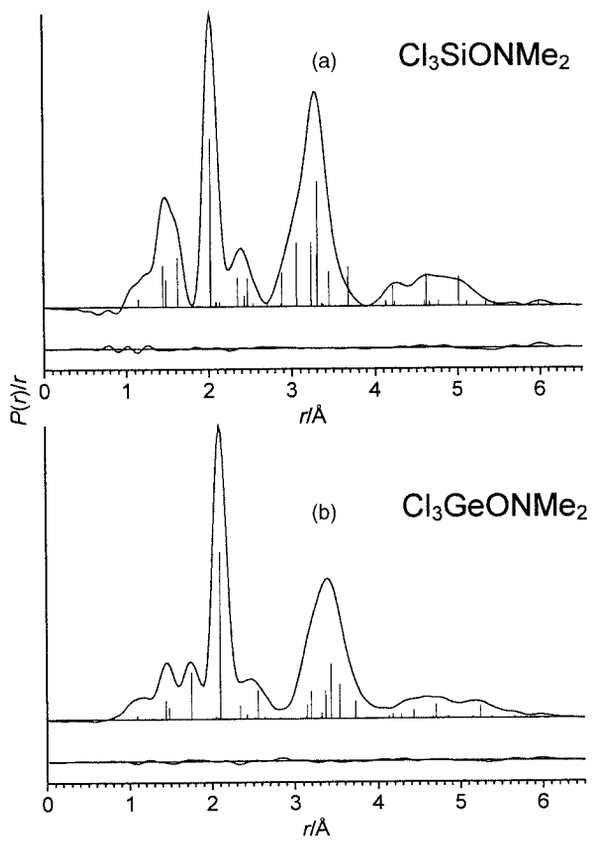

Fig. 4 Radial distribution and difference curve for the electron diffraction refinement of (a) $Cl_3SiONMe_2$ and (b) $Cl_3GeONMe_2$ (with the contribution of $GeCl_4$ subtracted). Before Fourier inversion the data were multiplied by $s{\cdot}\exp[(-0.002\ s^2)/(Z_E - f_E)(Z_{Cl} - f_{Cl})]$, E = Si, Ge. Vertical lines indicate atom pairs with their height being proportional to their scattering contribution.

E···N distances almost as short as the sum of the covalent radii of E and N, as is found in solid $ClH_2SiONMe_2$.

In Table 6 we see that the Si–O–N and Ge–O–N angles of $Cl_3SiONMe_2$ and $Cl_3GeONMe_2$ are in the same range as those of $Me_3SiONMe_2$ and $Me_3GeONMe_2$, the latter two having only marginally wider angles and slightly longer E···N distances. One might expect that the electrophilicity of the Cl_3Si and Cl_3Ge groups would lead to much smaller E···N distances associated with smaller Si–O–N and Ge–O–N angles. However, even in $H_3SiONMe_2$ a stronger attraction between Si and N atoms was observed.

Although most of the molecules under consideration here are comparatively small, a number of different effects play important roles in determining the strength of the E···N attractions. These include (i) electrostatic attraction between positively charged E and negatively charged N atoms, (ii) dipole–dipole and dipole–charge interactions, (iii) electron delocalisation of the types lp(N)→σ*(E–X) and lp(O)→σ*(E–X), (iv) the angle-bending potential at the oxygen atom and (v) steric repulsion

Table 6 Important geometrical parameter values (distances/Å, angles/°) for $Cl_3SiONMe_2$, $Cl_3GeONMe_2$ and E–O–N reference compounds (ave = averaged value; GED values all r_a)

Compound/method	E–O–N	E···N	Σ Bartell's radii
$Cl_3SiONMe_2$/GED	105.6(8)	2.473(12)	2.69
$Cl_3SiONMe_2$/XRD	103.0(ave)	2.437(ave)	2.69
$Cl_3GeONMe_2$/GED	104.0(11)	2.562(17)	2.72
$Me_3SiONMe_2$/GED	107.9(6)	2.566(8)	2.69
$Me_3GeONMe_2$/GED	108.9(7)	2.682(11)	2.72
$Me_3SnONMe_2$/GED	102.5(8)	2.731(14)	3.02
$Me_3SiON(CF_3)_2$/GED	113.4(19)	2.66	2.69
$MesF_2SiON(SiMe_3)_2$/XRD	117.66(11)	2.692	2.69
$ClH_2SiONMe_2$ (*anti*)/XRD	79.7(1)	2.028(1)	2.69
$ClH_2SiONMe_2$ (*anti*)/GED	87.1(9)	2.160(7)	2.69
$ClH_2SiONMe_2$ (*gauche*)/GED	104.7(11)	2.468(25)	2.69
$H_3SiONMe_2$/XRD	102.6	2.453	2.69
$H_2Si(ONMe_2)_2$/XRD	95.2(ave)	2.318(ave)	2.69

between the *gauche* substituents at E and the nitrogen substituents (Me).

In Table 7 a number of computational results are compiled including the E–O–N angles, the atomic charges at E, N and O and the shortest contacts between the atoms in silyl and germyl groups on one side and in the nitrogen substituents on the other side. For the compounds listed in this table, the charges on their N and O atoms vary only slightly, which is to be expected, as all compounds contain the same $ONMe_2$ group. The charge at the acceptor centre E is largely dependent on the nature of the substituents, with $F_3SiONMe_2$ being the most extreme case with $q(Si) = 1.80$ e. Although $F_3SiONMe_2$ is predicted to show the strongest E···N attraction, there is no obvious dependence of the strength of interaction and the charge on the acceptor centre, as $Cl_3SiONMe_2$ bears a markedly larger charge on silicon but has a larger Si–O–N angle than $ClH_2SiONMe_2$. This can be used as an argument against purely electrostatic attraction between E and N atoms as an explanation for the effect under investigation.

However, the compounds with the largest negative charge on nitrogen are those with the strongest E···N interactions. This accumulation of negative charge at nitrogen is inconsistent with the picture of a nitrogen centre donating electrons towards the acceptor atom, or as described in terms of natural orbital analysis with lp(N)→σ*(E–X) electron delocalisation. However, calculations for aminoboranes also predict the negative charge at the donor atom (nitrogen) to be slightly higher than in the free amine.[23]

The shortest distances between the *gauche* substituent at silicon and gemanium (Cl in the case of $Cl_3SiONMe_2$, H in the case of *anti*-$ClH_2SiONMe_2$) to the hydrogen atoms of the methyl groups at nitrogen should give an indication of the occurrence of repulsive forces between silyl or germyl groups on one side and methyl groups on the other, which would prevent shortening of the E···N distance, despite an attractive interaction between these centres. This could explain the large difference in the Si···N distances in $Cl_3SiONMe_2$ and $ClH_2SiONMe_2$. However, the data in Table 7 show that the Cl···H and H···H distances in $Cl_3SiONMe_2$ and $ClH_2SiONMe_2$ are considerably larger than the respective sums of van der Waals radii: the experimental value for the shortest Cl···H contact in $Cl_3GeONMe_2$ is 3.068(38) Å (the *ab initio* value is 2.994 Å), whereas the sum of the van der Waals radii is 2.80 Å. The repulsion in $Cl_3SiONMe_2$ could even be less pronounced if the possibility of weak hydrogen bonding between Cl and H is taken into consideration.

It should finally be noted that a more detailed consideration of orbital interaction is consistent with our experimental results. We performed a natural bond orbital analysis (NBO), despite the obvious deviations of theory from the experi-

Table 7 Computed Mulliken charges q (e), Si–O–N angles (°) and non-bonded distances (Å) between the silyl/germyl groups and the methyl units in $Cl_3SiONMe_2$, $Cl_3GeONMe_2$ and E–O–N reference compounds. For consistency all values are taken from fully optimised MP2(fc)/6-31G* calculations

Compound	SiON	q(Si/Ge)	q(N)	q(O)	Shortest contact		Σ v.d.W. radii
$Cl_3SiONMe_2$	100.4	1.18	−0.30	−0.60	Cl···H	3.012	2.8
$Cl_3GeONMe_2$	95.6	0.96	−0.26	−0.60	Cl···H	2.994	2.8
$F_3SiONMe_2$	86.5	1.80	−0.36	−0.59	F···H	2.65	2.4
$ClH_2SiONMe_2$ (*anti*)	88.9	1.06	−0.33	−0.61	H···H	2.70	2.0
$ClH_2SiONMe_2$ (*gauche*)	102.1	1.04	−0.28	−0.63	Cl···H	3.08	2.8
$H_3SiONMe_2$	99.9	0.92	−0.29	−0.65	H···H	2.92	2.0

Table 8 Experimental conditions (camera distances (mm), electron wavelengths (Å), nozzle and sample temperatures (°C)), data ranges and weighting functions (Å^{-1}), correlation parameters, scale factors and final R factors for the GED experiments and refinements of the compounds $Cl_3SiONMe_2$ and $Cl_3GeONMe_2$

Compound/ data set	Camera distance	Wavelength	T nozz	T samp	Δs	s_{min}	s_1	s_2	s_{max}	Correlation parameter	Scale factor	R_1	R_g
$Cl_3SiONMe_2$/1	285.47	0.06016	20	0	0.2	2.0	4.0	11.2	13.2	0.3650	0.850(5)	0.0388	0.0533
$Cl_3SiONMe_2$/2	128.08	0.06016	20	0	0.4	6.0	8.0	28.8	33.2	0.4116	0.890(14)	0.0700	
$Cl_3GeONMe_2$/1	285.47	0.06016	20	0	0.2	2.0	4.0	11.2	13.2	0.4842	0.840(5)	0.0574	0.0522
$Cl_3GeONMe_2$/2	128.08	0.06016	20	0	0.4	6.0	8.0	30.8	32.4	0.2903	0.850(10)	0.0469	

mentally obtained geometries. These calculations reveal many small contributions to electron delocalisation in these compounds. The most important to mention are those of the type lp(O)→σ*(E–X), which are common for Si–O and Ge–O compounds. A comparatively strong remote type of negative hyperconjugation, lp(N)→σ*(E–X), as was used to rationalise the nature of bonding in *anti*-$ClH_2SiONMe_2$, with its extremely small Si–O–N angle, is predicted to be present in $Cl_3SiONMe_2$ and $Cl_3GeONMe_2$, but in the latter two cases it makes a substantially smaller contribution. Although it is difficult to take all the contributions into concurrent consideration, it might be argued that the significant contributions of the type lp(Cl)→σ*(E–X) saturate the electrophilicity of the σ*(E–X) orbital positioned *anti* relative to the nitrogen lone pair, or to describe it in simpler terms, "backbonding" from the chlorine lone pairs to silicon reduces its electrophilic character.

Experimental

General

The experiments were carried out using a standard Schlenk line or a vacuum line with greaseless PTFE stopcocks (Young's taps), which was directly attached to the gas cell of an FTIR spectrometer (Midac Prospect FTIR). All NMR spectra were recorded at 21 °C on a JEOL JNM-LA400 spectrometer in sealed tubes with C_6D_6 as a solvent directly condensed onto the sample from K/Na alloy.

Syntheses

(*N*,*N*-Dimethylhydroxylamino)trichlorosilane. A solution of *N*,*N*-dimethylhydroxylamine (2.4 g, 40 mmol) and 2,6-dimethylpyridine (4.3 g, 40 mmol) in pentane (30 mL) was added dropwise to a solution of silicon tetrachloride (7.1 g, 42 mmol) in pentane (50 mL) at −55 °C. The mixture was slowly warmed to ambient temperature and all volatile products were separated from the remaining hydrochloride by repeated condensation. The product was separated in good yield (7.6 g, 32 mmol, 71%) by condensation through a series of cold traps held at −35, −60 and −196 °C, with the product retained at −60 °C. (*N*,*N*-Dimethylhydroxylamino)trichlorosilane is a colourless liquid (mp −55 °C) and extremely sensitive to moist air. ^{1}H NMR: δ 2.33 (s, 6H, H_3C). ^{13}C NMR: δ 49.2 (qq, $^1J_{CH}$ = 136.9 Hz, $^3J_{CNCH}$ = 5.1 Hz). ^{15}N NMR: δ −229.4 (sep, $^2J_{NCH}$ = 2.1 Hz). ^{17}O-{^{1}H} NMR: δ 161 (s). ^{29}Si NMR: δ −42.4 (s). GC-MS: m/z = 192 [M^+ − 1], 158 [M^+ − Cl], 133 [M^+ − $ON(CH_3)_2$]. $H_6C_2Cl_3NOSi$ (194.52 g mol^{-1}) calc.: C, 12.34; H, 3.11; N, 7.20. Found: C, 12.34; H, 3.66; N, 6.52%.

(*N*,*N*-Dimethylhydroxylamino)trichlorogermane. A solution of *N*,*N*-dimethylhydroxylamine (2.7 g, 45 mmol) and 2,6-dimethylpyridine (4.8 g, 45 mmol) in pentane (30 mL) was added dropwise to a solution of germanium tetrachloride (9.6 g, 45 mmol) in pentane (50 mL) at −55 °C. The mixture was slowly warmed to ambient temperature and all volatile products were separated from the remaining hydrochloride by repeated condensation. The product was separated in good yield (6.2 g, 32 mmol, 71%) by condensation through a series of cold traps held at −20, −60 and −196 °C, with the product retained at −60 °C. (*N*,*N*-Dimethylhydroxylamino)trichlorogermane is a colourless liquid, extremely sensitive to moist air and thermally unstable. ^{1}H NMR: δ 2.28 (s, 6H, H_3C). ^{13}C-{^{1}H} NMR: δ 49.84 (s, CH_3). ^{15}N-{^{1}H} NMR: δ −226.7 (s). ^{17}O-{^{1}H} NMR: δ 187 (s). IR: 2990, 2870 ν(CH), 1144 cm^{-1}.

Crystal structure determination of $Cl_3SiONMe_2$

A single crystal of $Cl_3SiONMe_2$ was grown *in situ* by slowly cooling the melt in a sealed capillary below the melting point after generation of a suitable seed crystal. $C_2H_6Cl_3NOSi$, M_r = 194.5, crystal system triclinic, space group $P2_1/c$, Z = 8, a = 11.585(1), b = 7.487(1), c = 19.069(2) Å, β = 98.37(1)°, V = 1636.4(3) Å^3 at 149(2) K, μ = 1.184 mm^{-1}. $2\theta_{max}$ = 56°, ω-scan, 3545 independent reflections [R_{int} = 0.032]. 187 parameters, R_1 = 0.0355 for 3532 reflections with $F_o > 4\sigma(F_o)$ and wR_2 = 0.1029 for all 3532 data.

CCDC reference number 186/1696.

See http://www.rsc.org/suppdata/dt/1999/4291/ for crystallographic files in .cif format.

Gas-phase electron diffraction

Electron scattering intensity data for $Cl_3SiONMe_2$ and $Cl_3GeONMe_2$ were recorded on Kodak Electron Image plates using the Edinburgh electron diffraction apparatus.[24] The samples were held at 0 °C and the inlet nozzle at 20 °C during the experiments. Scattering data for benzene were recorded concurrently and used to calibrate the electron wavelength and camera distances. Three exposures were taken at each camera distance. Data were obtained in digital form using the microdensitometer at the Royal Greenwich Observatory at Cambridge.[25] The experimental conditions and data ranges are listed in Table 8.

The data analysis followed standard procedures, using established data reduction and least-squares refinement programs[26] and the scattering factors established by Fink and co-workers.[27] The refined molecular parameters, their definition and the applied restraints, a list of selected interatomic distances including vibrational amplitudes and applied restraints, and elements of the correlation matrix are given Tables 3, 4 and supplementary data.

Ab initio calculations

Ab initio molecular orbital calculations were carried out using the Gaussian 98 program.[28] Geometry optimisations and vibrational frequency calculations were performed from analytic first and second derivatives at the SCF and MP2 levels of theory. Calculations were undertaken at the SCF level using the standard 3-21G*[29] and 6-31G*[30] basis sets, while the larger was used for calculations at the MP2 level of theory. NBO calculations were undertaken with the NBO 3.0 facilities built into Gaussian 98.

Acknowledgements

This work was supported by the Bayerisches Staatsministerium für Wissenschaft, Forschung und Kunst (Bayerischer Habilitationsförderpreis 1996 for N. W. M.), the Deutsche Forschungsgemeinschaft, the Fonds der Chemischen Industrie, the Leonhard-Lorenz-Stiftung and EPSRC (Grant No. GR/K44411). Generous support by Professor H. Schmidbaur (Garching) is gratefully acknowledged.

References

1 (*a*) R. R. Holmes, *Chem. Rev.*, 1990, **90**, 17; (*b*) C. Chuit, R. J. P. Corriu, C. Reyé and J. C. Young, *Chem. Rev.*, 1993, **93**, 1371.
2 R. Tacke, D. Reichel, M. Kropfgans, P. G. Jones, E. Mutschler, J. Gross, X. Hou, M. Waeldbrock and G. Lambrecht, *Organometallics*, 1995, **14**, 251.
3 (*a*) M. G. Voronkov, V. M. Dyakov and S. V. Kirpichenko, *J. Organomet. Chem.*, 1982, **233**, 1; (*b*) M. W. Schmidt, T. L. Windus and M. S. Gordon, *J. Am. Chem. Soc.*, 1995, **117**, 7480.
4 N. W. Mitzel, U. Losehand and A. Richardson, *Organometallics*,1999, **18**, 2610.
5 N. W. Mitzel and U. Losehand, *Angew. Chem.*, *Int. Ed. Engl.*, 1997, **36**, 2807.
6 N. W. Mitzel and U. Losehand, *J. Am. Chem. Soc.*, 1998, **120**, 7320.
7 P. Nowakovski and R. West, *J. Am. Chem. Soc.*, 1976, **98**, 5616.
8 Y. Hamada and S. Mori, *Proceedings of the 29th Organosilicon Symposium*, Evanston, IL, March 1996.
9 R. A. Murphy, *Fr. Pat.*, 1462725, 1966; *Chem. Abstr.*, 1967, **67**, 54258.
10 M. G. Voronkov, E. A. Maletina and V. K. Roman, *Heterosiloxanes Vol. 2*, *Derivatives of Nitrogen and Phosphorus*, Harwood Academic Publishers GmbH, Chur, Switzerland, 1991.
11 (*a*) M. G. Voronkov, V. P. Feshin, V. F. Mironov, S. A. Mikhailyants and T. K. Gar, *Zh. Obshch. Khim.*, 1971, **41**, 2211; (*b*) M. G. Voronkov, T. V. Kashik, E. Y. Lukevits, E. S. Deriglazova, A. E. Pestunovich and R. Y. Moskovich, *Zh. Obshch. Khim.*, 1974, **44**, 2211.
12 N. W. Mitzel, C. Kiener and D. W. H. Rankin, *Organometallics*, 1999, **18**, 3437.
13 (*a*) K. Wieghard, I. Tolksdorf, J. Weiss and W. Swiridoff, *Z. Anorg. Allg. Chem.*, 1982, **490**, 182; (*b*) N. W. Mitzel, S. Parsons, A. J. Blake and D. W. H. Rankin, *J. Chem. Soc.*, *Dalton Trans.*, 1996, 2089.
14 T. Hertel, J. Jakob, R. Minkwitz and H. Oberhammer, *Inorg. Chem.*, 1998, **37**, 5092.
15 R. Wolfgramm, U. Klingebiel and M. Noltemeyer, *Z. Anorg. Allg. Chem.*, 1998, **624**, 856.
16 U. Losehand and N. W. Mitzel, *Eur. J. Inorg. Chem.*, 1998, 2023.
17 (*a*) A. J. Blake, P. T. Brain, H. McNab, J. Miller, C. A. Morrison, S. Parsons, D. W. H. Rankin, H. E. Robertson and B. A. Smart, *J. Phys. Chem.*, 1996, **100**, 12280; (*b*) N. W. Mitzel, B. A. Smart, A. J. Blake, H. E. Robertson and D. W. H. Rankin, *J. Phys. Chem.*, 1996, **100**, 9339.
18 L. S. Bartell, D. J. Romenensko and T. C. Wong, *Mol. Struct. Diffr. Methods*, 1975, **3**, 72.
19 V. J. Klimkowski, J. D. Ewbank, C. Van Alsenoy, J. N. Scarsdale and L. Schäfer, *J. Am. Chem. Soc.*, 1982, **104**, 1476.
20 (*a*) W. Airey, C. Glidewell, A. G. Robiette and G. M. Sheldrick, *J. Mol. Struct.*, 1971, **8**, 413; (*b*) M. Yokoi, *Bull. Chem. Soc. Jpn.*, 1957, **30**, 100; (*c*) K. Yamasaki, A. Kotera, M. Yokoi and Y. Ueda, *J. Chem. Phys.*, 1950, **18**, 1414.
21 W. Airey, C. Glidewell, D. W. H. Rankin, A. G. Robiette, G. M. Sheldrick and D. W. J. Cruickshank, *Trans. Faraday Soc.*, 1970, **66**, 551.
22 (*a*) L. S. Bartell, *J. Chem. Phys.*, 1960, **32**, 827; (*b*) C. Glidewell, *Inorg. Chim. Acta*, 1975, **12**, 219.
23 A. Haaland, *Angew. Chem.*, *Int. Ed. Engl.*, 1989, **28**, 992.
24 C. M. Huntley, G. S. Laurenson and D. W. H. Rankin, *J. Chem. Soc.*, *Dalton Trans.*, 1980, 945.
25 J. R. Lewis, P. T. Brain and D. W. H. Rankin, *Spectrum*, 1997, **15**, 7.
26 N. W. Mitzel, P. T. Brain and D. W. H. Rankin, ED96, Version 2.0, 1998. A program developed on the basis of formerly described ED programs: A. S. F. Boyd, G. Laurenson and D. W. H. Rankin, *J. Mol. Struct.*, 1981, **71**, 217.
27 A. W. Ross, M. Fink and R. Hilderbrandt, *International Tables for X-Ray Crystallography*, ed. A. J. C. Wilson, Kluwer Academic Publishers, Dordrecht, Boston, 1992, vol. C, p. 245.
28 Gaussian 98, Revision A.6, M. J. Frisch, G. W. Trucks, H. B. Schlegel, G. E. Scuseria, M. A. Robb, J. R. Cheeseman, V. G. Zakrzewski, J. A. Montgomery, Jr., R. E. Stratmann, J. C. Burant, S. Dapprich, J. M. Millam, A. D. Daniels, K. N. Kudin, M. C. Strain, O. Farkas, J. Tomasi, V. Barone, M. Cossi, R. Cammi, B. Mennucci, C. Pomelli, C. Adamo, S. Clifford, J. Ochterski, G. A. Petersson, P. Y. Ayala, Q. Cui, K. Morokuma, D. K. Malick, A. D. Rabuck, K. Raghavachari, J. B. Foresman, J. Cioslowski, J. V. Ortiz, B. B. Stefanov, G. Liu, A. Liashenko, P. Piskorz, I. Komaromi, R. Gomperts, R. L. Martin, D. J. Fox, T. Keith, M. A. Al-Laham, C. Y. Peng, A. Nanayakkara, C. Gonzalez, M. Challacombe, P. M. W. Gill, B. Johnson, W. Chen, M. W. Wong, J. L. Andres, C. Gonzalez, M. Head-Gordon, E. S. Replogle and J. A. Pople, Gaussian, Inc., Pittsburgh, PA, 1998.
29 (*a*) J. S. Binkley, J. A. Pople and W. J. Hehre, *J. Am. Chem. Soc.*, 1980, **102**, 939; (*b*) M. S. Gordon, J. S. Binkley, J. A. Pople, W. J. Pietro and W. J. Hehre, *J. Am. Chem. Soc.*, 1982, **104**, 2797; (*c*) W. J. Pietro, M. M. Francl, W. J. Hehre, D. J. Defrees, J. A. Pople and J. S. Binkley, *J. Am. Chem. Soc.*, 1982, **104**, 5039.
30 (*a*) W. J. Hehre, R. Ditchfield and J. A. Pople, *J. Chem. Phys.*, 1972, **56**, 2257; (*b*) P. C. Hariharan and J. A. Pople, *Theor. Chim. Acta*, 1973, **28**, 213.
31 J. D. Odom, E. J. Stampf, Y. S. Li and J. R. Durig, *J. Mol. Struct.*, 1978, **49**, 1.

Paper 9/06688H